Radiology

Post-Acute Sequelae of COVID-19 Pneumonia: Six-month Chest CT Follow-up

Damiano Caruso, MD, PhD • Gisella Guido, MD • Marta Zerunian, MD • Tiziano Polidori, MD • Elena Lucertini, MD • Francesco Pucciarelli, MD • Michela Polici, MD • Carlotta Rucci, MD • Benedetta Bracci, MD • Matteo Nicolai, MD • Antonio Cremona, MD • Chiara De Dominicis, MD • Andrea Laghi, MD

From the Department of Surgical and Medical Sciences and Translational Medicine, Sapienza University of Rome-Sant'Andrea University Hospital, Via di Grottarossa, 1035-1039, 00189 Rome, Italy. Received March 28, 2021; revision requested April 9; revision received May 6; accepted May 10. **Address correspondence to** A.L. (e-mail: *andrea.laghi@uniroma1.it*).

Conflicts of interest are listed at the end of this article.

See also the editorial by Wells and Devaraj in this issue.

Radiology 2021; 301:E396–E405 • https://doi.org/10.1148/radiol.2021210834 • Content code: CH

Background: The long-term post-acute pulmonary sequelae of COVID-19 remain unknown.

Purpose: To evaluate lung injury in patients affected by COVID-19 pneumonia at the 6-month follow-up CT examination compared with the baseline chest CT examination.

Materials and Methods: From March 19, 2020, to May 24, 2020, patients with moderate to severe COVID-19 pneumonia who had undergone baseline chest CT were prospectively enrolled at their 6-month follow-up. The CT qualitative findings, semiquantitative Lung Severity Score (LSS), and the well-aerated lung volume at quantitative chest CT (QCCT) analysis were analyzed. The performance of the baseline LSS and QCCT findings for predicting fibrosis-like changes (reticular pattern and/or honeycombing) at the 6-month follow-up chest CT examination was tested by using receiver operating characteristic curves. Univariable and multivariable logistic regression analyses were used to test clinical and radiologic features that were predictive of fibrosis-like changes. The multivariable analysis was performed with clinical parameters alone (clinical model), radiologic parameters alone (radiologic model), and the combination of clinical and radiologic parameters (combined model).

Results: One hundred eighteen patients who had undergone baseline chest CT and agreed to undergo follow-up chest CT at 6 months were included in the study (62 women; mean age, 65 years ± 12 [standard deviation]). At follow-up chest CT, 85 of 118 (72%) patients showed fibrosis-like changes and 49 of 118 (42%) showed ground-glass opacities. The baseline LSS (>14) and QCCT findings (≤3.75 L and ≤80%) showed excellent performance for predicting fibrosis-like changes at follow-up chest CT. In the multivariable analysis, the areas under the curve were 0.89 (95% CI: 0.77, 0.96) for the clinical model, 0.81 (95% CI: 0.68, 0.9) for the radiologic model, and 0.92 (95% CI: 0.81, 0.98) for the combined model.

Conclusion: At 6-month follow-up chest CT, 72% of patients showed late sequelae, in particular fibrosis-like changes. The baseline Lung Severity Score and the well-aerated lung volume at quantitative chest CT (QCCT) analysis showed excellent performance for predicting fibrosis-like changes at the 6-month chest CT (area under the curve, >0.88). Male sex, cough, lymphocytosis, and the well-aerated lung volume at QCCT analysis were significant predictors of fibrosis-like changes at 6 months, demonstrating an inverse correlation (area under the curve, 0.92).

COVID-19 is caused by a novel coronavirus known as SARS-CoV-2 and was declared a pandemic by the World Health Organization on March 11, 2020 (1). Chest CT qualitative findings of COVID-19 pneumonia have been deeply investigated in the literature (2), as have quantitative chest CT (QCCT) methods (3–5) and semiquantitative Lung Severity Scores (LSSs) (6,7). Typical chest CT findings of COVID-19 pneumonia include bilateral and multilobe ground-glass opacities (GGOs) with posterior and peripheral distribution associated with consolidations, interlobular septal thickening, and enlargement of both subsegmental pulmonary arteries and veins (>3 mm) (8).

The short- and midterm chest CT outcomes in patients with COVID-19 (9,10) have been reported in some studies, which used both qualitative and semiquantitative methods (11–13); fibrosis was a common finding at a few weeks from the onset of the symptoms (14–16). A recent study (17) demonstrated that approximately one-third of survivors of COVID-19 showed pulmonary fibrosis–like changes at the 6-month follow-up chest CT. Nevertheless, as a novel pathologic entity, further long-term investigations are needed to obtain a comprehensive knowledge of COVID-19 pulmonary sequelae. Indeed, there is great concern that some of these findings will resolve over time and are therefore not fibrotic (18).

In fact, for other severe viral pneumonias that arose previously, several studies demonstrated that long-term lung impairment is a common sequela (19); among them, the long-term follow-up studies on severe acute respiratory syndrome by Zhang et al (20) and Wu et al (21) demonstrated persistent pulmonary interstitial damage several months after recovery.

Thus, the aims of our study were to prospectively investigate late sequelae at the 6-month follow-up chest CT examination in patients affected by COVID-19 pneumonia, to compare these CT features with those present at the baseline chest CT examination, and to evaluate the role of

Abbreviations

AUC = area under the curve, GGO = ground-glass opacity, LSS = Lung Severity Score, OR = odds ratio, QCCT = quantitative chest CT

Summary

At 6-month follow-up chest CT, COVID-19 post-acute sequelae were detected in 72% of patients: fibrosis-like changes were the most common residual findings (72%), which were followed in prevalence by ground-glass opacities (42%).

Key Results

- The baseline Lung Severity Score (>14) showed optimal performance for predicting fibrosis-like changes at follow-up (area under the curve [AUC], 0.91; sensitivity, 88%; specificity, 80%).
- Multivariable analysis showed that male sex, cough, lymphocytosis, and the well-aerated lung volume at quantitative chest CT analysis were significant predictors of fibrosis-like changes at the 6-month follow-up, demonstrating an inverse correlation (AUC, 0.92; sensitivity, 100%; specificity, 73%).

chest CT and clinical parameters in predicting pulmonary fibrosis–like changes at the 6-month follow-up.

Materials and Methods

Patient Population and Study Design

This prospective study was approved by our local institutional review board, and written informed consent was obtained from all study participants. Patients admitted to Sant'Andrea University Hospital, Rome, Italy, from March 19, 2020, to May 24, 2020, who met both of the following inclusion criteria were prospectively enrolled for a 6-month follow-up chest CT evaluation: *(a)* patients with a diagnosis of moderate to severe COVID-19 (22) that was confirmed by using reverse transcription polymerase chain reaction analysis and who had undergone chest CT, and *(b)* patients with a diagnosis of interstitial pneumonia who had undergone a baseline chest CT scan with positive results that was performed at admission.

To define the severity of COVID-19 pneumonia, the World Health Organization's interim guidance diagnostic criteria for adults with severe COVID-19 pneumonia were used (22). Exclusion criteria were as follows: *(a)* patient death during the follow-up interval, *(b)* refusal of the patient to undergo follow-up chest CT, and *(c)* severe motion artifacts at the first chest CT examination.

On the day of the follow-up CT examination, all patients filled out a questionnaire about the long-lasting symptoms after COVID-19 and smoking habits; the oxygen saturation level was also measured and recorded for each patient. Patients' demographic characteristics, clinical findings, laboratory results, and the use of eventual ventilation support and corticosteroid therapy during the hospitalization were also retrieved from the internal hospital records.

CT Acquisition Technique

All patients underwent 6-month (±14 days [standard deviation]) follow-up unenhanced chest CT scans. Chest CT acquisitions were obtained with the patients in a supine position during end-inspiration and without contrast medium injection. Chest CT was performed with a 128-section CT scanner (Revolution EVO, GE Medical Systems). The following technical parameters were used: tube voltage, 120 kV; tube current modulation, 100–250 mAs; spiral pitch factor, 0.98; and collimation width, 0.625. Reconstructions were made by using a convolution kernel Bone Plus algorithm at a section thickness of 1.25 mm.

Qualitative Analysis

Digital Imaging and Communications in Medicine data were transferred into a picture archiving and communication system workstation (Centricity Universal Viewer, version 6.0; GE Medical Systems). Two radiologists in consensus (A.C. and C.D.D., with 5 years and 20 years in thoracic imaging experience, respectively) qualitatively analyzed chest CT images and evaluated the presence of motion artifacts. The following CT findings were recorded: GGOs, GGO pattern, GGO location, multilobe involvement, total lobar involvement, bilateral distribution, posterior involvement by consolidations or GGOs, consolidation, interlobular septal thickening, fibrosis-like changes (reticular pattern and/or honeycombing) (23), bronchiectasis, air bronchogram, bronchial wall thickening, pulmonary nodules surrounded by GGOs, halo sign or reversed halo sign, pleural and pericardial effusion, lymphadenopathy (defined as a lymph node with a short axis >10 mm), enlargement of subsegmental arteries and veins (<3 mm), and pulmonary trunk diameter (<31 mm). All mentioned chest CT findings were defined as in the Fleischner Society glossary (24).

LSS Analysis

The presence of GGOs, consolidation, and fibrosis-like changes were semiquantitatively analyzed in consensus by the same two radiologists mentioned above, who used the LSS (ranging from 0–40 points), which has previously been used in the literature to quantify COVID-19 pneumonia lung impairment (25). Ten segments for each lung were considered; each segment was evaluated and received 0–2 points on the basis of the area involved, with a score of 0 indicating normal parenchyma, a score of 1 indicating less than 50% segmental involvement, and a score of 2 indicating up to 50% segmental involvement. The final LSS was obtained from the sum of all lung segments; furthermore, individual segmental scores were added together to generate a total score with which to perform the statistical analysis.

Quantification Chest CT Analysis

Two other radiologists in consensus (G.G. and D.C., with 3 years and 7 years of experience in thoracic imaging, respectively) performed QCCT analysis to quantify the well-aerated lung volume by using dedicated software (Thoracic VCAR, version 13.1; GE Medical Systems). An attenuation value less than −1000 HU was used to exclude tracheal air from the analysis before segmentation. To select well-aerated lung volumes for software segmentation, a range between −950 HU and −700 HU of attenuation was selected (26–28). The software automatically calculated the healthy lung volume, which was expressed both as a percentage and in liters. In cases of unsatisfactory or incorrect lung segmentation, the radiologists manually adjusted the lung contours.

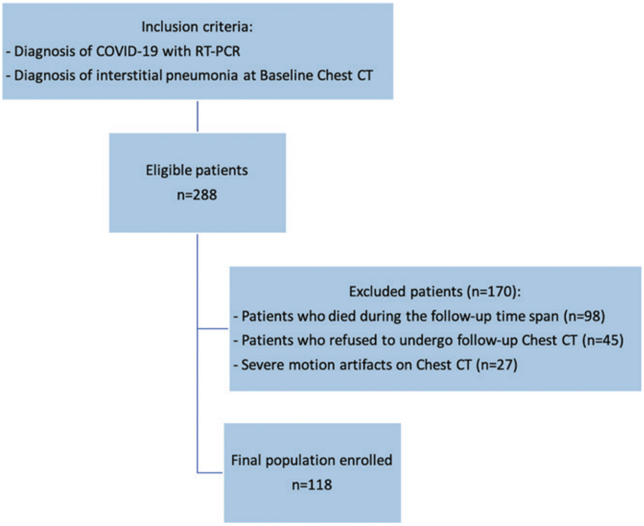

Figure 1: Enrollment flowchart of the study. From an initial cohort of 288 patients, 118 patients who had undergone both baseline and 6-month follow-up chest CT were enrolled. RT-PCR = reverse transcription polymerase chain reaction.

Statistical Analysis

Statistical analysis was performed by using SPSS (version 21.0, IBM) and MedCalc Statistical Software (version 17.9.7, MedCalc Software). *P* values less than .05 were considered to indicate statistical significance. All data are expressed as the mean ± standard deviation. Categorical variables were described as counts and percentages; a comparison of the qualitative CT findings was performed by using the χ^2 test. The comparison between the baseline and follow-up LSSs and between the well-aerated lung volumes at QCCT analysis were tested by using a Student *t* test for data with a Gaussian distribution; otherwise, a Wilcoxon test was applied.

Receiver operating characteristic curves and the areas under the curve (AUCs) were calculated to test the performance of the baseline LSS and QCCT findings for predicting fibrosis-like changes at the 6-month follow-up chest CT examination.

Univariable and backward multivariable logistic regression analyses were used to test clinical and radiologic features as predictors of fibrosis-like changes at the 6-month follow-up. At first, univariable analysis was individually performed on the variables of age, sex, and comorbidities (dichotomized by presence and absence); smoking habits (dichotomized by current and former smokers grouped together and never-smokers); the baseline clinical parameters of cough, dyspnea, fever, C-reactive protein level, D-dimer level, lactate dehydrogenase level, lymphocytes, oxygen saturation level, and ventilation support; and the baseline radiologic variables of LSS, pulmonary bilateral involvement, consolidations, and the well-aerated lung volume at QCCT analysis (expressed in liters and as a percentage). The multivariable analysis was performed on three different models. The clinical model included age, sex, comorbidities, smoking habits, cough, dyspnea, fever, C-reactive protein, D-dimer level, lactate dehydrogenase level, lymphocytes, oxygen saturation level at admission, and ventilation support; the radiologic model contained the LSS, pulmonary bilateral involvement, consolidations, and the well-aerated lung volume at QCCT analysis (expressed in liters and as a percentage); and, finally, the combined model comprised all of these parameters.

Table 1: Patient Demographic, Smoking, Comorbidity, and Treatment Data (*n* = 118)

Characteristic	Data
Mean age (y)	65 ± 12
Age range (y)	37–84
Male	56 (47)
Female	62 (53)
Smoking habits	
Current smoker	24 (20)
Ex-smoker	27 (23)
Never-smoker	67 (57)
Comorbidities	82 (69)
Hypertension	40 (34)
Cardiovascular disease	18 (15)
Diabetes mellitus	11 (9)
Other	13 (11)
Ventilatory treatment	
No	31 (26)
Yes	87 (74)
NIV*	53 (61)
Duration (d)	2 ± 0.6
IMV*	34 (39)
Duration (d)	11.3 ± 3.6
Corticosteroid therapy	
No	7 (6)
Yes	111 (94)

Note.—Data are means ± standard deviations, range, or number of patients with the percentage in parentheses. IMV = invasive mechanical ventilation, NIV = noninvasive ventilation.

* Percentages are calculated on the basis of the total number of patients who received ventilatory treatment.

Results

Patient Population, Clinical Data, and Laboratory Findings

From an initial population of 288 patients, 98 (34%) died during the follow-up period, 45 (16%) refused the follow-up chest CT examination because it had already been performed elsewhere, and 27 (9%) patients were excluded for the presence of severe motion artifacts on chest CT images obtained at admission. Thus, the final population comprised 118 patients, 56 of whom were men (48%), with a mean age of 65 years ± 12 (range, 37–84 years). The enrollment flowchart of the study is showed in Figure 1.

Twenty-four of 118 (20%) patients had a current smoking habit, 27 of 118 (23%) had quit tobacco, and 67 of 118 (57%) had never smoked. Twenty-four of 118 patients (20%) had one underlying comorbidity, whereas 58 of 118 patients (49%) had two or more comorbidities; common comorbidities included hypertension (40 of 118 patients [34%]), cardiovascular diseases (18 of 118 patients [15%]), and diabetes mellitus (11 of 118 patients [9%]).

Ninety-one of 118 patients (77%) reported persistent or new symptoms, including cough (22 of 91 [24%]), dyspnea (38 of 91 [42%]), fatigue (seven of 91 [8%]), gastrointestinal symptoms (15 of 91 [16%]), hair loss (18 of 91 [20%]), a decline of visual acuity

Table 2: Patient Laboratory Findings, Signs, and Symptoms (*n* = 118)

Parameter	Baseline	Follow-up
Blood test results		
Lymphocytopenia demonstrated by lymphocyte count <1.1 × 10^9/L	65 (55)	27 (23)
CRP increased by >0.50 mg/dL	102 (86)	5 (4)
LDH increased by >220 U/L	94 (80)	34 (29)
D-dimer increased by >500 ng/mL	31 (26)	28 (24)
Signs and symptoms		
Oxygen saturation (%)	94.6 ± 2.95	96.9 ± 1.97
Symptomatic*	111 (94)	91 (77)
Dyspnea	49 (44)	38 (42)
Cough	51 (46)	22 (24)
Fever	89 (80)	0 (0)
GI symptoms	20 (18)	15 (17)
Fatigue	88 (79)	7 (8)
Olfactory dysfunction	68 (61)	13 (14)
Gustatory dysfunction	55 (50)	18 (20)
Hair loss	0 (0)	18 (20)
Decline of visual acuity	0 (0)	11 (12)
Asymptomatic	7 (6)	27 (23)

Note.—Data are the number of patients with the percentage in parentheses or the mean ± standard deviation. CRP = C-reactive protein, GI = gastrointestinal, LDH = lactate dehydrogenase.

* Percentages for individual symptoms are calculated on the basis of the total number of symptomatic patients.

(11 of 91 [12%]), and olfactory and gustatory dysfunctions (13 of 91 [14%] and 18 of 91 [20%], respectively); 27 of 118 patients (23%) were asymptomatic, and the mean oxygen saturation level was 97% ± 1.97.

Full data about patients' demographics, clinical records, laboratory findings, and eventual ventilation support and corticosteroid therapy are reported in Tables 1 and 2.

Qualitative Analysis

At the 6-month chest CT follow-up, 33 of 118 (28%) patients presented with normal lung findings. Eighty-five of 118 (72%) patients presented with fibrosis-like changes, and 49 of 118 (42%) patients presented with GGOs, which were peripheral in distribution in 40 of 118 (34%) patients. Multilobe involvement (two or more lobes) was observed in 45 of 118 (38%) patients, and involvement of all lobes was observed in 16 of 118 (14%) patients. Interstitial septal thickening was detected in 33 of 118 (28%) patients, and consolidative opacities were observed in two of 118 patients (2%).

All chest CT findings were reduced at the follow-up chest CT, except for the presence of fibrosis-like changes, which was the only feature showing a significant increase (all $P < .05$). The full results from the follow-up chest CT examinations and the comparison with the baseline chest CT findings are shown in Table 3. Examples of chest CT images obtained at baseline and the 6-month follow-up are shown in Figures 2 and 3.

Table 3: Comparison between Baseline and Follow-up Chest CT Findings in Patients with COVID-19

CT Finding	Baseline	Six-month Follow-up	*P* Value
GGO pattern	102 (86)	49 (42)	<.001
Predominantly linear	54 (46)	47 (40)	.38
Round	24 (20)	2 (2)	<.001
Crazy paving	24 (20)	0 (0)	<.001
GGO location (peripheral)	96 (81)	40 (34)	<.001
Multilobe involvement (two or more lobes)	96 (81)	45 (38)	<.001
Total lobar involvement	80 (68)	16 (14)	<.001
Bilateral distribution	94 (80)	33 (28)	<.001
Posterior (lung) involvement by GGO and/or consolidation	94 (80)	16 (14)	<.001
Consolidative opacities	80 (68)	2 (2)	<.001
Interlobular septal thickening	62 (53)	33 (28)	.007
Fibrosis-like changes	65 (55)	85 (72)	<.001
Bronchiectasis	40 (34)	29 (25)	.23
Air bronchogram	38 (32)	0 (0)	<.001
Bronchial wall thickening	36 (31)	5 (4)	<.001
Pulmonary nodules surrounded by GGOs	18 (15)	0 (0)	<.001
Halo sign	11 (9)	0 (0)	.002
Reversed halo sign	11 (9)	0 (0)	.08
Pericardial effusion	27 (23)	16 (14)	.13
Pleural effusion	20 (17)	2 (2)	<.001
Lymphadenopathy	31 (26)	5 (4)	<.001
Enlargement, subsegmental arteries and veins (≥3 mm)	109 (92)	82 (69)	.07
Pulmonary trunk diameter (<31 mm)	98 (83)	98 (83)	.99

Note.—Data are the number of patients with the percentage in parentheses. *P* values less than .05 indicate statistical significance. GGO = ground-glass opacity.

LSS Analysis

At the 6-month follow-up, the summed LSS was 4.37 ± 5.29 (range, 0–20; LSSs in right and left lungs of 2.15 ± 2.68 and 2.22 ± 2.79, respectively), showing a significant decrease compared with the summed baseline LSS of 15.34 ± 8.32 (range, 0–30; LSSs in the right and left lungs of 7.58 ± 4.13 and 7.75 ± 4.71, respectively) (all $P < .001$). A per-segment analysis was also performed, and the results fully reported in Table 4.

QCCT Analysis

The results of the 6-month follow-up QCCT analysis of the well-aerated lung volume expressed as a percentage and in liters were 82% ± 12.27 and 3.84 L ± 1.34, respectively, showing significant differences compared with the baseline values (69% ± 18.2 and 2.99 L ± 1.5; all $P < .001$). An example of the well-aerated lung volume at baseline and the comparison with the well-aerated lung volume at follow-up QCCT analysis is provided in Figure 4.

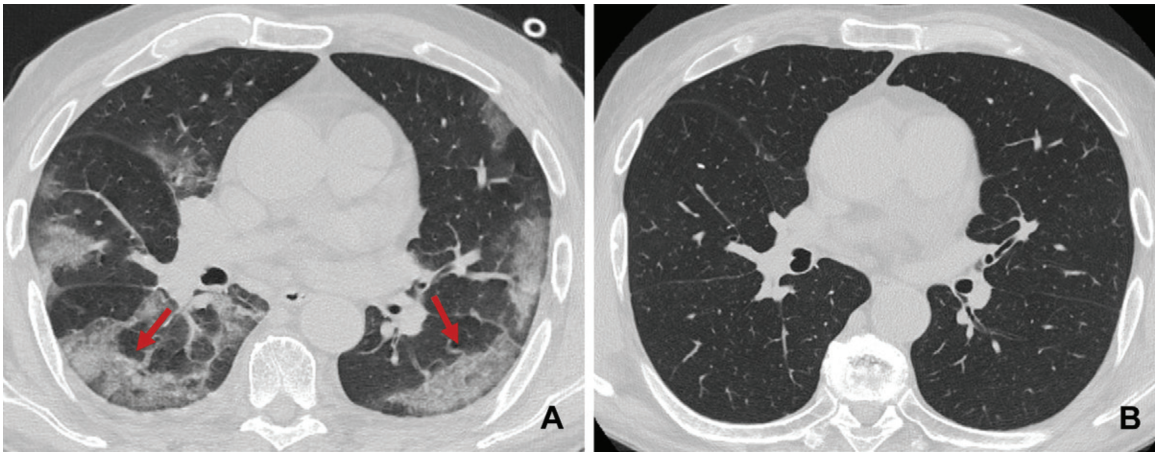

Figure 2: Baseline and 6-month follow-up axial thin-section unenhanced chest CT images in an 83-year-old man, a former smoker, who presented with fever, cough, and worsening dyspnea; COVID-19 was confirmed by using reverse transcription polymerase chain reaction testing. **(A)** The baseline image shows multiple bilateral and confluent ground-glass opacities with a predominantly linear pattern and a peripheral distribution (arrows). **(B)** The 6-month follow-up image shows complete resolution of ground-glass opacities without fibrosis-like changes.

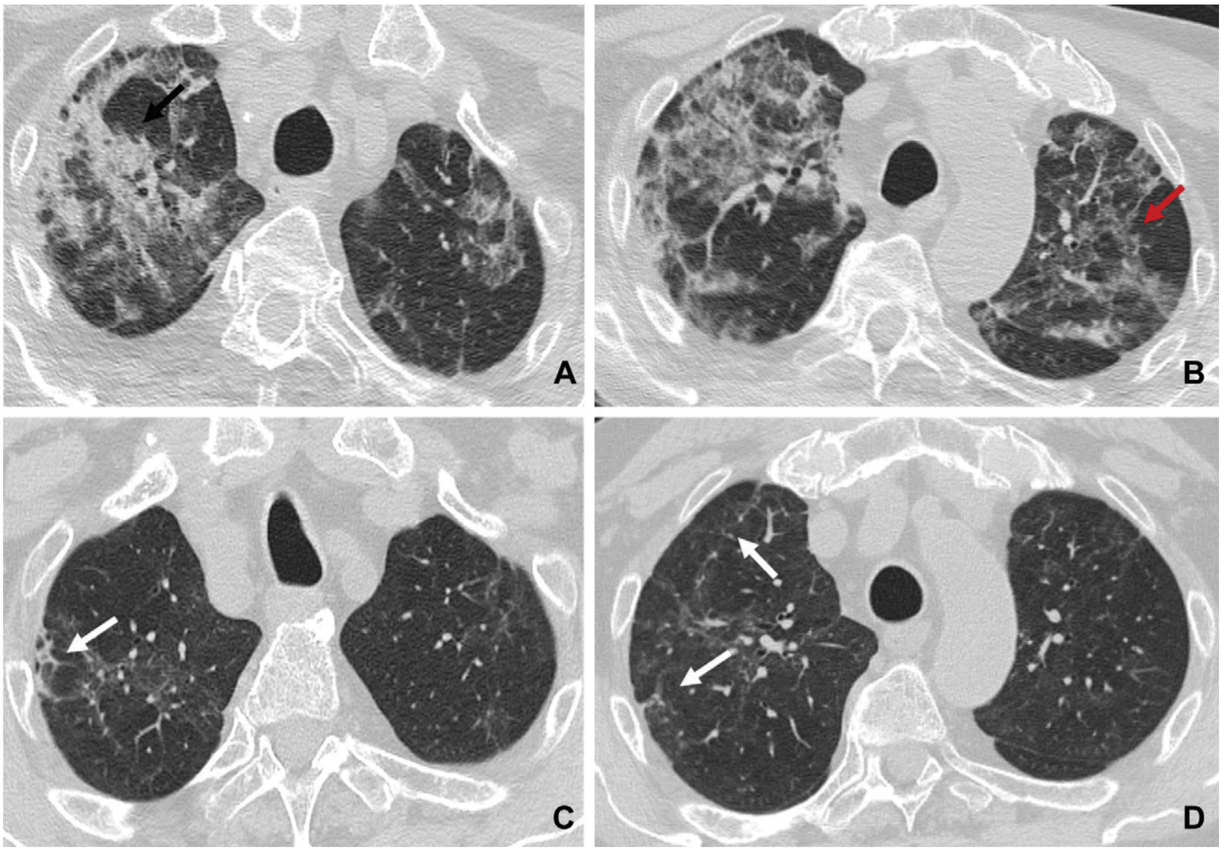

Figure 3: Baseline and 6-month follow-up axial thin-section unenhanced chest CT images in an 84-year-old man, a current smoker, admitted to the emergency department presenting with fever and cough; COVID-19 was confirmed by using reverse transcription polymerase chain reaction testing. **(A, B)** The baseline images show bilateral consolidative pulmonary opacities (black arrow) with diffuse ground-glass opacities and interstitial septal thickening (red arrow). **(C, D)** The 6-month follow-up images show residual ground-glass opacities with decreased opacity compared with those at baseline, interstitial septal thickening, and peripheral fibrosis-like changes (arrows).

Receiver Operating Characteristic Curves and Logistic Regression

The baseline LSS showed excellent performance for predicting fibrosis-like changes at the 6-month chest CT follow-up, demonstrating an AUC of 0.91 (95% CI: 0.8, 0.97), a sensitivity of 88%, and a specificity of 80% when the LSS cutoff was greater than 14. The baseline QCCT analysis of the well-aerated lung volume showed an AUC of 0.88 (95% CI: 0.77, 0.96), a sensitivity of 86%, and a specificity of 80% when expressed in liters (cutoff of ≤3.75 L) and showed an AUC

Table 4: Comparison between Baseline and Follow-up LSS

Parameter	Baseline	Follow-up	*P* Value*
Total LSS			
Total sum	15.3 ± 8.32	4.37 ± 5.29	<.001
Right lung sum	7.58 ± 4.13	2.15 ± 2.68	<.001
Left lung sum	7.75 ± 4.71	2.22 ± 2.79	<.001
Right lung segment LSS			
Anterior	0.73 ± 0.52	0.15 ± 0.36	<.001
Apical	0.6 ± 0.49	0.18 ± 0.39	<.001
Posterior	0.9 ± 0.63	0.16 ± 0.37	<.001
Medial	0.56 ± 0.6	0.18 ± 0.39	.001
Lateral	0.71 ± 0.6	0.22 ± 0.42	<.001
Superior	0.88 ± 0.64	0.22 ± 0.42	<.001
Anterior basal	0.54 ± 0.53	0.11 ± 0.32	<.001
Medial basal	0.62 ± 0.59	0.24 ± 0.43	<.001
Lateral basal	0.88 ± 0.61	0.24 ± 0.43	<.001
Posterior basal	1.11 ± 0.64	0.39 ± 0.53	<.001
Left lung segment LSS			
Anterior	0.75 ± 0.58	0.13 ± 0.34	<.001
Apical	0.56 ± 0.5	0.22 ± 0.42	<.001
Posterior	0.96 ± 0.67	0.15 ± 0.36	<.001
Superior lingular	0.84 ± 0.63	0.18 ± 0.39	<.001
Inferior lingular	0.73 ± 0.59	0.34 ± 0.47	<.001
Superior	0.84 ± 0.72	0.2 ± 0.41	<.001
Anterior basal	0.67 ± 0.64	0.17 ± 0.38	<.001
Medial basal	0.6 ± 0.56	0.24 ± 0.43	.001
Lateral basal	0.79 ± 0.63	0.26 ± 0.44	<.001
Posterior basal	0.96 ± 0.58	0.3 ± 0.5	<.001

Note.— Lung Severity Scores (LSSs) are shown as the mean ± standard deviation. Summed scores are the sum of all applicable segmental scores (score of 0–2).
* *P* values less than .05 indicate statistical significance.

of 0.88 (95% CI: 0.76, 0.95), a sensitivity of 74%, and a specificity of 100% when expressed as a percentage (cutoff of ≤80%), as shown in Figure 5.

In the univariable analysis, age older than 65 years (odds ratio [OR], 1.1; 95% CI: 1.03, 1.17; *P* = .004) and the baseline LSS (OR, 1.15; 95% CI: 1.05, 1.25; *P* = .003) were proven to be significant positive independent predictors of fibrosis-like changes at the 6-month follow-up chest CT examination (all *P* < .05). On the other side, male sex (OR, 0.33; 95% CI: 0.92, 1.14; *P* = .002), an oxygen saturation of 96%–97% (OR, 0.13; 95% CI: 0.02, 0.95; *P* = .04), the absence of the need for ventilation (OR, 0.16; 95% CI: 0.04, 0.63; *P* = .008), bilateral lung involvement (OR, 0.28; 95% CI: 0.06, 0.92; *P* = .04), the presence of pulmonary consolidations (OR, 0.27; 95% CI: 0.08, 0.96; *P* = .04), and the baseline well-aerated lung volume at QCCT analysis expressed in liters (OR, 0.4; 95% CI: 0.22, 0.71; *P* = .002) and as a percentage (OR, 0.93; 95% CI: 0.88, 0.99; *P* = .01) showed a significant inverse correlation with the presence of fibrosis-like changes at the 6-month follow-up chest CT examination (all *P* < .05).

In the multivariable clinical model analysis, the best positive predictors of fibrosis-like changes at the 6-month follow-up chest CT examination were an age older than 65 years (OR, 1.12; 95% CI: 1.03, 1.21; *P* = .007) and the need for mechanical ventilation (OR, 14.02; 95% CI: 1.07, 185.55; *P* = .04). Otherwise, the radiologic model showed an inverse correlation between the quantified well-aerated lung volume and fibrosis-like changes (OR, 0.4; 95% CI: 0.22, 0.71; *P* = .002). Finally, the combined model showed that male sex (OR, 0.03; 95% CI: 0.001, 0.89; *P* = .04), cough (OR, 0.08; 95% CI: 0.01, 0.88; *P* = .04), lymphocytosis (OR, 0.08; 95% CI: 0.01, 0.86; *P* = .04), and the well-aerated lung volume at QCCT analysis expressed in liters (OR, 0.05; 95% CI: 0.01, 1.19; *P* = .03) were significant predictors of fibrosis-like changes at the 6-month follow-up, with an inverse correlation being shown. The full results of the univariable and multivariable logistic regression analyses are shown in Table 5.

The diagnostic performance of the three models is reported in Figure 6. For the clinical model, the AUC was 0.89 (95% CI: 0.77, 0.96; sensitivity, 82%; specificity, 93%); for the radiologic model, the AUC was 0.81 (95% CI: 0.68, 0.9; sensitivity, 84%; specificity, 67%); and for the combined model, the AUC was 0.92 (95% CI: 0.81, 0.97; sensitivity, 100%; specificity, 73%). Even though the clinical model had already performed well, the combined model was analyzed as well to fully investigate the possibility of obtaining stronger results with data derived from different fields of investigation.

Discussion

The results of our study showed that 72% of patients presented with fibrosis-like changes at the 6-month follow-up chest CT examination and that the baseline Lung Severity Score (>14) was an excellent predictor of fibrosis-like changes (area under the curve [AUC], 0.91). Furthermore, in the multivariable analysis, a model combining clinical and radiologic findings achieved excellent diagnostic performance (AUC, 0.92). In this model, male sex, cough, lymphocytosis, and the well-aerated lung volume at quantitative chest CT analysis expressed in liters showed an inverse correlation with lung fibrosis-like changes.

Although the clinical model had already performed well (AUC, 0.89), we decided to additionally analyze the combined model to fully investigate the possibility of obtaining stronger results with data derived from different fields of investigation.

The percentage of patients with late sequelae in our population at the 6-month follow-up chest CT examination (72%) is in agreement with the findings from the study conducted by Zhao et al (75%) (10), who found that the most common feature at 3-month follow-up was interstitial septal thickening (27% vs 28% in our study). On the other hand, our results differ from those of Tabatabaei et al (9), who reported residual CT findings in 42% of patients examined at the 3-month follow-up; among them, 55% presented with residual GGOs (42%). These different results may be related to the younger age of their population and the lower percentage of patients who were hospitalized in

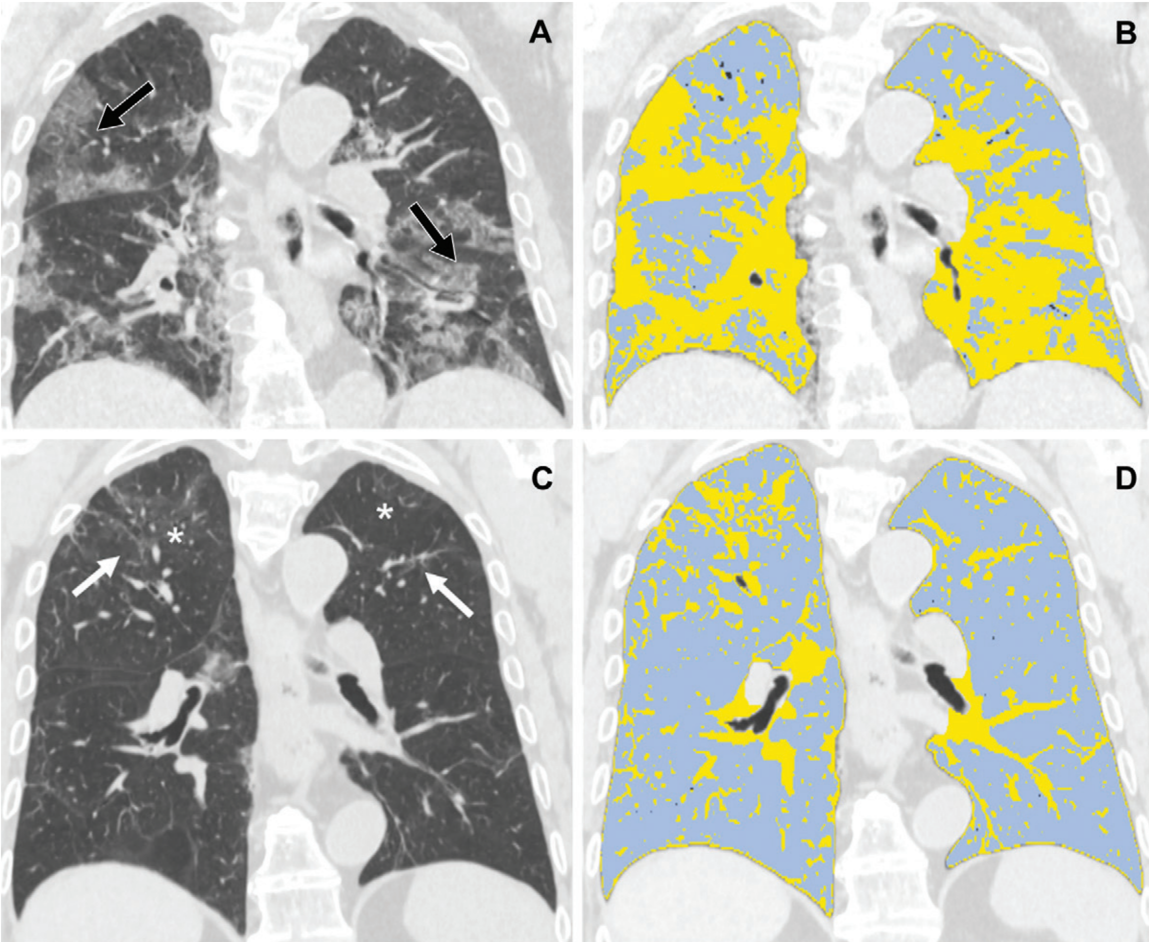

Figure 4: Baseline and 6-month follow-up coronal thin-section unenhanced chest CT images in a 79-year-old man admitted to the emergency department presenting with fever, dyspnea, and cough; COVID-19 was confirmed by using reverse transcription polymerase chain reaction testing. **(A)** Chest CT image shows bilateral ground-glass opacities tending toward consolidation (arrows). **(B)** The same image after quantitative chest CT analysis shows the well-aerated lung volume (1.5 L, 50%) in light blue and pulmonary injury due to COVID-19 pneumonia in yellow. **(C)** The 6-month follow-up CT image shows residual fibrosis-like changes (arrows) and the persistence of low-opacity ground glass (asterisks). **(D)** The same image after quantitative chest CT analysis shows the well-aerated lung volume (3.5 L, 82%) in light blue and residual findings of COVID-19 pneumonia in yellow at the 6-month follow-up.

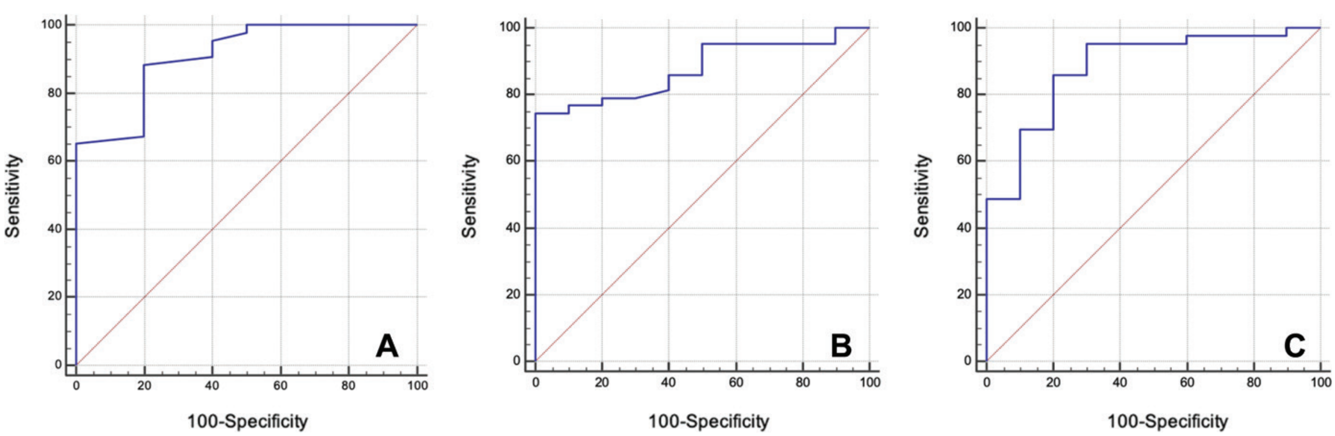

Figure 5: **(A)** Receiver operating characteristic (ROC) curves are used to test the performance of the baseline Lung Severity Score to predict fibrosis-like changes at the 6-month follow-up chest CT examination, showing an area under the curve (AUC) of 0.91 (95% CI: 0.8, 0.9), a sensitivity of 88%, and a specificity of 80% when the cutoff is greater than 14. **(B, C)** ROC curves are used to test the performance of the baseline well-aerated lung volume at quantitative chest CT (QCCT) analysis for predicting fibrosis-like changes at the 6-month follow-up chest CT examination, demonstrating an AUC of 0.88 (95% CI: 0.77, 0.96), a sensitivity of 86%, and a specificity of 80% when the volume is expressed in liters with a cutoff of less than or equal to 3.8 L **(B)** and demonstrating an AUC of 0.88 (95% CI: 0.76, 0.95), a sensitivity of 74%, and a specificity of 100% when the volume is expressed as a percentage with a cutoff of less than or equal to 80% **(C)**.

Table 5: Univariable and Multivariable Logistic Regression Analyses

	Univariable Analysis		Clinical Model		Radiologic Model		Combined Model	
Variable	Odds Ratio	*P* Value	Odds Ratio	*P* Value	Odds Ratio	*P* Value	Odds Ratio	*P* Value
Age	1.1 (1.03, 1.17)	.004	1.12 (1.03, 1.21)	.007	…	…	…	…
Sex = 0*	0.33 (0.92, 1.14)	.002	…	…	…	…	0.03 (0.001, 0.89)	.04
Comorbidities	…	…	…	…	…	…	…	…
Smoker†	…	…	…	…	…	…	…	…
Cough = 1‡	…		…	…	…	…	0.08 (0.01, 0.88)	.04
Dyspnea	…	…	…	…	…	…	…	…
Fever	…	…	…	…	…	…	…	…
CRP	1.11 (0.99, 1.25)	.07	…	…	…	…	…	…
D-dimer	…	…	…	…	…	…	…	…
LDH	1.01 (0.99, 1.01)	.07	…	…	…	…	…	…
Lymphocytes	…	…	…	…	…	…	0.08 (0.01, 0.86)	.04
Oxygen saturation of 96%	0.13 (0.02, 0.95)	.04	…	…	…	…	…	…
Oxygen saturation of 97%	0.13 (0.02, 0.94)	.04	…	…	…	…	…	…
Ventilation = 1§	0.16 (0.04, 0.63)	.008	…	…	…	…	…	…
Ventilation = 3‖	NA	NA	14.09 (1.07, 185.55)	.04	NA	NA	NA	NA
NIV duration (d)	NA	NA	NA	NA	NA	NA	NA	NA
IMV duration (d)	NA	NA	NA	NA	NA	NA	NA	NA
LSS	1.15 (1.05, 1.25)	.003	NA	NA	NA	NA	NA	NA
Bilateral involvement	0.23 (0.06, 0.92)	.03	NA	NA	NA	NA	NA	NA
Consolidation	0.27 (0.08, 0.96)	.04	NA	NA	NA	NA	NA	NA
Well-aerated lung volume								
Expressed in liters	0.4 (0.22, 0.71)	.002	NA	NA	0.4 (0.22, 0.71)	.002	0.44 (0.01, 1.19)	.03
Expressed as percentage	0.93 (0.88, 0.99)	.01	NA	NA	NA	NA	NA	NA

Note.—Data in parentheses are 95% CIs. The analyses show the relationship between the clinical and radiologic variables in 118 patients with moderate to severe COVID-19 at the 6-month follow-up CT examination. *P* values less than .05 are considered to indicate statistical significance. The Cox-Snell R^2 = 0.45 for the combined model. CRP = C-reactive protein, IMV = invasive mechanical ventilation, LDH = lactate dehydrogenase, LSS = Lung Severity Score, NA = not applicable, NIV = noninvasive ventilation.

* Sex = 0 indicates male.

† Current and former smokers were grouped together.

‡ Cough = 1 indicates cough present.

§ Ventilation = 1 indicates no ventilation needed.

‖ Ventilation = 3 indicates IMV needed.

an intensive care unit, compared with our older population of patients who needed ventilation support at a higher rate during hospitalization. In fact, the older age of our population increased the need for ventilation support and might be related to more aggressive damage of the lung parenchyma, consequently resulting in a higher percentage of our population having late sequelae (29). Further studies of the long-term effects in patients with COVID-19 are necessary for confirming this hypothesis.

A remarkable 6-month follow-up study performed by Han et al (17) showed that approximately one-third (35%) of survivors of COVID-19 had pulmonary fibrosis–like changes, whereas 62% of patients presented with GGOs. In our population, fibrosis-like changes did not arise de novo but evolved from GGOs and/or consolidations.

Discrepancies with our results might be related to demographic differences such as the prevalence of male patients and younger patients, although demographic data on fibrosis development are still lacking and confirmation on chest CT images is therefore needed within a larger population sample. In addition, all non–fibrosis-like abnormalities were reduced at 6 months, probably because almost all of our patients had received steroid therapy during hospitalization.

Because COVID-19 is a novel disease, it is crucial to perform risk stratification of patients with COVID-19 at the baseline stage to identify who will be at high risk of developing residual disease thereafter. In fact, recent studies have found that a semiquantitative chest CT score is a useful tool for stratifying the severity of pneumonia and for predicting clinical and radiologic outcomes in patients with COVID-19 at short-term follow-up (9,10,30). Our baseline LSS showed optimal performance for predicting residual findings at follow-up chest CT (AUC, 0.91); 76 patients (64%) presented with a baseline LSS higher than

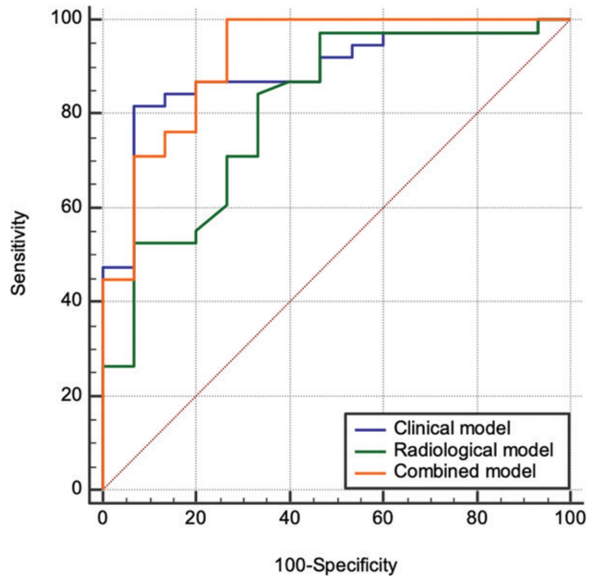

Figure 6: Receiver operating characteristic curves are used to test the performance of the clinical model (blue line), radiologic model (green line), and combined model (orange line) for predicting the presence of fibrosis-like changes at the 6-month follow-up chest CT examination. The clinical model shows an area under the curve (AUC) of 0.89 (95% CI: 0.77, 0.96), a sensitivity of 82%, and a specificity of 93%. The radiologic model shows an AUC of 0.81 (95% CI: 0.68, 0.9), a sensitivity of 84%, and a specificity of 67%. The combined model shows an AUC of 0.92 (95% CI: 0.81, 0.97), a sensitivity of 100%, and a specificity of 73%.

14. This result supports the findings of similar analyses conducted at the 3-month follow-up by Tabatabaei et al (9) and Zhao et al (10), who demonstrated that patients with residual lung disease had a significantly higher CT severity score than the group with completely recovered lungs. In addition, the total chest CT scores obtained by Han et al (17) showed a correlation with pulmonary fibrosis–like changes at the 6-month follow-up chest CT examination, despite some differences between the two lung scoring systems used.

Likewise, the baseline well-aerated lung volume at QCCT analysis demonstrated good performance for predicting residual findings at the follow-up chest CT examination, both when expressed in liters (AUC, 0.88) and when expressed as a percentage (AUC, 0.88). Our results concerning the role of the well-aerated lung volume at QCCT analysis support the findings of previous studies conducted by Colombi et al (27), who showed that a low well-aerated lung volume was a predictor of intensive care unit admission or death, and Lanza et al (31), who demonstrated that a compromised lung volume was a predictor of the need for oxygen support, the need for intubation, and patient death.

In line with the study conducted at short-term follow-up by Yu et al (14), we found that older age is a potential predictor of fibrosis-like changes at 6 months. Moreover, we found that fibrosis-like changes at the chest CT follow-up were more frequent in women. In previous midterm follow-up studies (9,10), no significant correlation between sex and follow-up fibrosis-like changes was found (32).

Despite the encouraging results, our study had some limitations. These included the relatively small sample size, the potential selection bias due to patients' refusal to undergo follow-up CT at our hospital because of follow-up CT already having been performed in other centers, and the lack of an analysis of inter- and intrareader agreement.

In conclusion, at the 6-month follow-up, 72% of patients showed late sequelae, particularly fibrosis-like changes. The baseline Lung Severity Score and well-aerated lung volume at quantitative chest CT (QCCT) analysis showed excellent performance for predicting fibrosis-like changes at the 6-month chest CT follow-up (area under the curve [AUC], >0.88). Male sex, cough, lymphocytosis, and the well-aerated lung volume at QCCT analysis in liters were significant predictors of fibrosis-like changes at 6 months, demonstrating an inverse correlation (AUC, 0.92).

Author contributions: Guarantors of integrity of entire study, all authors; study concepts/study design or data acquisition or data analysis/interpretation, all authors; manuscript drafting or manuscript revision for important intellectual content, all authors; approval of final version of submitted manuscript, all authors; agrees to ensure any questions related to the work are appropriately resolved, all authors; literature research, D.C., G.G., M.Z., T.P., E.L., F.P., M.P., C.R., B.B., M.N., C.D.D.; clinical studies, D.C., G.G., A.C.; statistical analysis, D.C., G.G., F.P.; and manuscript editing, D.C., G.G., M.Z., T.P., E.L., M.P., C.R., B.B., M.N., A.C., C.D.D., A.L.

Disclosures of Conflicts of Interest: **D.C.** disclosed no relevant relationships. **G.G.** disclosed no relevant relationships. **M.Z.** disclosed no relevant relationships. **T.P.** disclosed no relevant relationships. **E.L.** disclosed no relevant relationships. **F.P.** disclosed no relevant relationships. **M.P.** disclosed no relevant relationships. **C.R.** disclosed no relevant relationships. **B.B.** disclosed no relevant relationships. **M.N.** disclosed no relevant relationships. **A.C.** disclosed no relevant relationships. **C.D.D.** disclosed no relevant relationships. **A.L.** disclosed payment for lectures including service on speakers bureaus from Bracco, GE Healthcare, MSD, and Bayer.

References

1. Naming the coronavirus disease (COVID-19) and the virus that causes it. World Health Organization Web site. https://www.who.int/emergencies/diseases/novel-coronavirus-2019/technical-guidance/naming-the-coronavirus-disease-(covid-2019)-and-the-virus-that-causes-it. Published 2020. Accessed August 19, 2021.
2. Caruso D, Zerunian M, Polici M, et al. Chest CT Features of COVID-19 in Rome, Italy. Radiology 2020;296(2):E79–E85.
3. Huang L, Han R, Ai T, et al. Serial quantitative chest CT assessment of COVID-19: a deep learning approach. Radiol Cardiothorac Imaging 2020;2(2):e200075.
4. Caruso D, Polici M, Zerunian M, et al. Quantitative chest CT analysis in discriminating COVID-19 from non-COVID-19 patients. Radiol Med (Torino) 2021;126(2):243–249.
5. Shen C, Yu N, Cai S, et al. Quantitative computed tomography analysis for stratifying the severity of coronavirus disease 2019. J Pharm Anal 2020;10(2):123–129.
6. Chung M, Bernheim A, Mei X, et al. CT imaging features of 2019 novel coronavirus (2019-nCoV). Radiology 2020;295(1):202–207.
7. Zhan J, Li H, Yu H, et al. 2019 Novel coronavirus (COVID-19) pneumonia: CT manifestations and pattern of evolution in 110 patients in Jiangxi, China. Eur Radiol 2021;31(2):1059–1068.
8. Caruso D, Polidori T, Guido G, et al. Typical and atypical COVID-19 computed tomography findings. World J Clin Cases 2020;8(15):3177–3187.
9. Tabatabaei SMH, Rajebi H, Moghaddas F, Ghasemiadl M, Talari H. Chest CT in COVID-19 pneumonia: what are the findings in mid-term follow-up? Emerg Radiol 2020;27(6):711–719.
10. Zhao YM, Shang YM, Song WB, et al. Follow-up study of the pulmonary function and related physiological characteristics of COVID-19 survivors three months after recovery. EClinicalMedicine 2020;25:100463.
11. Hu Q, Guan H, Sun Z, et al. Early CT features and temporal lung changes in COVID-19 pneumonia in Wuhan, China. Eur J Radiol 2020;128:109017.
12. Huang G, Gong T, Wang G, et al. Timely diagnosis and treatment shortens the time to resolution of coronavirus disease (COVID-19) pneumonia and lowers the highest and last CT scores from sequential chest CT. AJR Am J Roentgenol 2020;215(2):367–373.

13. Liu N, He G, Yang X, et al. Dynamic changes of chest CT follow-up in coronavirus disease-19 (COVID-19) pneumonia: relationship to clinical typing. BMC Med Imaging 2020;20(1):92.
14. Yu M, Liu Y, Xu D, Zhang R, Lan L, Xu H. Prediction of the development of pulmonary fibrosis using serial thin-section CT and clinical features in patients discharged after treatment for COVID-19 pneumonia. Korean J Radiol 2020;21(6):746–755.
15. Ojha V, Mani A, Pandey NN, Sharma S, Kumar S. CT in coronavirus disease 2019 (COVID-19): a systematic review of chest CT findings in 4410 adult patients. Eur Radiol 2020;30(11):6129–6138.
16. Salehi S, Abedi A, Balakrishnan S, Gholamrezanezhad A. Coronavirus disease 2019 (COVID-19): a systematic review of imaging findings in 919 patients. AJR Am J Roentgenol 2020;215(1):87–93.
17. Han X, Fan Y, Alwalid O, et al. Six-month follow-up chest CT findings after severe COVID-19 pneumonia. Radiology 2021;299(1):E177–E186.
18. Wells AU, Devaraj A, Desai SR. Interstitial lung disease after COVID-19 infection: a catalog of uncertainties. Radiology 2021;299(1):E216–E218.
19. Salehi S, Reddy S, Gholamrezanezhad A. Long-term pulmonary consequences of coronavirus disease 2019 (COVID-19): what we know and what to expect. J Thorac Imaging 2020;35(4):W87–W89.
20. Zhang P, Li J, Liu H, et al. Long-term bone and lung consequences associated with hospital-acquired severe acute respiratory syndrome: a 15-year follow-up from a prospective cohort study. Bone Res 2020;8(1):8 [Published correction appears in Bone Res 2020;8:34.].
21. Wu X, Dong D, Ma D. Thin-section computed tomography manifestations during convalescence and long-term follow-up of patients with severe acute respiratory syndrome (SARS). Med Sci Monit 2016;22:2793–2799.
22. Clinical management of severe acute respiratory infection (SARI) when COVID-19 disease is suspected. World Health Organization Web site. https://www.who.int/docs/default-source/coronaviruse/clinical-management-of-novel-cov.pdf. Published March 13, 2020. Accessed August 19, 2021.
23. Hansell DM, Goldin JG, King TE Jr, Lynch DA, Richeldi L, Wells AU. CT staging and monitoring of fibrotic interstitial lung diseases in clinical practice and treatment trials: a position paper from the Fleischner Society. Lancet Respir Med 2015;3(6):483–496.
24. Hansell DM, Bankier AA, MacMahon H, McLoud TC, Müller NL, Remy J. Fleischner Society: glossary of terms for thoracic imaging. Radiology 2008;246(3):697–722.
25. Yang R, Li X, Liu H, et al. Chest CT severity score: an imaging tool for assessing severe COVID-19. Radiol Cardiothorac Imaging 2020;2(2):e200047.
26. Chen A, Karwoski RA, Gierada DS, Bartholmai BJ, Koo CW. Quantitative CT analysis of diffuse lung disease. RadioGraphics 2020;40(1):28–43.
27. Colombi D, Bodini FC, Petrini M, et al. Well-aerated lung on admitting chest CT to predict adverse outcome in COVID-19 pneumonia. Radiology 2020;296(2):E86–E96.
28. Vernuccio F, Giambelluca D, Cannella R, et al. Radiographic and chest CT imaging presentation and follow-up of COVID-19 pneumonia: a multicenter experience from an endemic area. Emerg Radiol 2020;27(6):623–632.
29. Chen Y, Klein SL, Garibaldi BT, et al. Aging in COVID-19: vulnerability, immunity and intervention. Ageing Res Rev 2021;65:101205.
30. Lyu P, Liu X, Zhang R, Shi L, Gao J. The performance of Chest CT in evaluating the clinical severity of COVID-19 pneumonia: identifying critical cases based on CT characteristics. Invest Radiol 2020;55(7):412–421.
31. Lanza E, Muglia R, Bolengo I, et al. Quantitative chest CT analysis in COVID-19 to predict the need for oxygenation support and intubation. Eur Radiol 2020;30(12):6770–6778.
32. Gebhard C, Regitz-Zagrosek V, Neuhauser HK, Morgan R, Klein SL. Impact of sex and gender on COVID-19 outcomes in Europe. Biol Sex Differ 2020;11(1):29.